The Figure of Merit "C" for Comparing Superresolution Direction-Finding Algorithms

Harry Commin and Athanassios Manikas
Department of Electrical and Electronic Engineering, Imperial College London
South Kensington Campus, London, SW7 2AZ, UK
harry.commin@imperial.ac.uk
a.manikas@imperial.ac.uk

***Abstract*—In this paper, the parameter C is introduced as a figure of merit for comparing the performances of practical direction-finding (DF) algorithms in terms of their superresolution capabilities. C takes values between 0 and 1, with higher values indicating better resolving capability and $C = 1$ denotes an algorithm with the theoretically ideal resolution performance.**

Analytical expressions for C can be derived for a number of DF algorithms. In this paper, three such expressions are derived for MUSIC, 'optimal' Beamspace MUSIC and Minimum Norm. It is found that optimal beamspace MUSIC yields the smallest resolution separation, which can approach the ideal when incident signals have equal powers.

NOTATION

a, A	Scalar
$\underline{a}, \underline{A}$	Column Vector
$\mathbb{A}, \mathbf{A}$	Matrix
$(\cdot)^T$	Transpose
$(\cdot)^H$	Conjugate transpose
$\mathbb{I}_N$	$(N \times N)$ identity matrix
$\lvert\cdot\rvert$	Absolute value
$\lVert\cdot\rVert$	Euclidean norm of vector
$\exp(\underline{a})$	Element-by-element exponential

I. INTRODUCTION

The resolution performance of an array system is, in general, a function of array aperture and number of sensors, N. In practice, these resources are limited and so the purpose of a superresolution DF algorithm is to achieve high resolution performance without increasing the size of the array. In particular, algorithms which belong to this category have asymptotically infinite resolving capability as the number of data snapshots, L, becomes large. Superresolution techniques have therefore been an important research topic for several decades [1].

Since the number of snapshots available in practice is finite, the estimated statistics of the noise-contaminated received signal are imperfect. This finite sampling effect therefore imposes limits on system performance. Specifically, theoretical bounds on three key aspects of DF performance arise:

1) Detection Performance: the capability of a system to correctly estimate the number of signals, M, impinging on the array.
2) Resolution Performance: the capability of a system to yield M separate, distinct directional parameter estimates corresponding to the M impinging signals.
3) Estimation Accuracy: the mean square error of the directional parameter estimates (which can only be obtained following successful detection and resolution), with respect to true target directions.

In the case of detection and resolution, overall success depends particularly on the two most closely-spaced sources. Detection and resolution performance can therefore each be characterised by a different 'threshold' separation, which must be satisfied in order for detection/resolution to be achieved with high probability. These thresholds are dependent upon various system parameters such as: signal-to-noise ratio (SNR), L, N, array geometry, source bearings, relative source powers, signal correlation and the specific practical DF algorithm employed.

In this paper, the parameter C is introduced in order to characterise the impact of practical DF algorithms on resolution performance. It therefore serves as a useful figure of merit for comparing the relative resolving capabilities of different superresolution DF algorithms. In Section III, resolution bounds are examined and the parameter C is derived in general terms. In Section IV, specific analytical expressions for C are derived and discussed for the MUSIC, optimal Beamspace MUSIC and Minimum Norm algorithms for uncorrelated signals. Finally, the paper is concluded in Section V.

II. ARRAY SIGNAL MODEL

Consider M narrow-band plane wave signals impinging on an array of N sensors. The $(N \times 1)$ received signal vector at the array output (in the presence of noise) can be modelled as follows:

$$\underline{x}(t) = \mathbb{S}(\underline{\theta}, \underline{\phi})\underline{m}(t) + \underline{n}(t) \tag{1}$$

where $\underline{m}(t)$ is the M-vector of the baseband source signals, $\underline{n}(t)$ is additive noise and $\mathbb{S}(\underline{\theta}, \underline{\phi})$ is the manifold matrix, having the following structure:

$$\mathbb{S}(\underline{\theta}, \underline{\phi}) = [\underline{S}(\theta_1, \phi_1), \underline{S}(\theta_2, \phi_2), \ldots, \underline{S}(\theta_M, \phi_M)] \tag{2}$$

with parameter vectors $\underline{\theta} = [\theta_1, \theta_2, \ldots, \theta_M]^T$ and $\underline{\phi} = [\phi_1, \phi_2, \ldots, \phi_M]^T$ denoting the directional parameters associated with the M sources (e.g. azimuth and elevation, where azimuth is measured anti-clockwise from the positive x-axis). The $(N \times 1)$ complex vector $\underline{S}(\theta, \phi)$ is the array manifold vector (array response vector):

$$\underline{S}(\theta, \phi) \triangleq \exp\left(-j\mathbf{r}\,\underline{k}(\theta, \phi)\right) \tag{3}$$

of the source signal impinging from (θ, ϕ). In Equation 3, the array geometry is represented by the $(N \times 3)$ real matrix:

$$\mathbf{r} \triangleq [\underline{r}_x, \underline{r}_y, \underline{r}_z] = [\underline{r}_1, \underline{r}_2, \ldots, \underline{r}_N]^T \in \mathcal{R}^{N\times 3} \tag{4}$$

and $\underline{k}(\theta, \phi)$ is the wavenumber vector:

$$\underline{k}(\theta, \phi) \triangleq \frac{2\pi}{\lambda}\underline{u}(\theta, \phi) \tag{5}$$

where λ is the signal wavelength and $\underline{u}(\theta, \phi)$ is the (3×1) real unit vector pointing from (θ, ϕ) towards the origin.

III. Theoretical Resolution Bounds

For a given array, the array manifold is defined as the locus of the manifold vectors for all (θ, ϕ) across the whole parameter space. In the presence of finite sampling effects, the uncertainty remaining in the system (corresponding to a given point on the manifold) after L snapshots can be represented using an N-dimensional hypersphere:

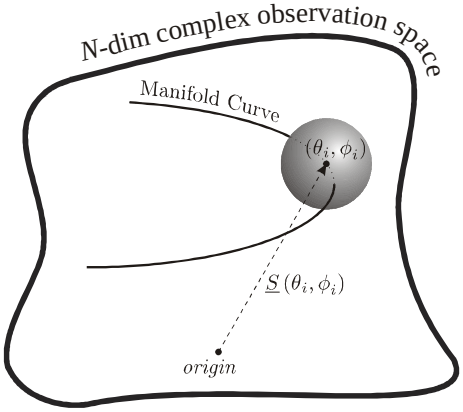

Fig. 1: Visualisation of an uncertainty hypersphere in an N-dimensional complex space.

It has been proven in [2, Ch. 8, p. 199] that if the directional parameters, (θ, ϕ), are expressed as a function of the arc length of the manifold curve, then the radius, σ_e, of the uncertainty hypersphere is given by the square root of the single-source Cramer-Rao Lower Bound expressed in terms of the arc length of the manifold:

$$\sigma_e = \frac{1}{\sqrt{2\,(\mathrm{SNR} \times L)\,C}} \tag{6}$$

where any additional uncertainty introduced by the practical DF algorithm is contained within the parameter C (with $0 < C \leq 1$), which scales the hypersphere accordingly. Evidently, $C = 1$ denotes the theoretically ideal algorithm, which introduces no additional uncertainty and eliminates any dependency which may exist between the parameters of the received signal. Lower values of C reflect poorer algorithm performance. Thus, C provides a useful figure of merit for comparing the relative performances of different DF algorithms.

Based on this hyperspheres model, there are two laws which provide the theoretical detection and resolution bounds [2]. Specifically, as a function of $(\mathrm{SNR} \times L)$, the threshold source separations, $\Delta p \triangleq |p_2 - p_1|$, are given by the square root law for detection and fourth root law for resolution:

$$\Delta p_{det-thr} = \frac{1}{\dot{s}\left(\frac{p_1+p_2}{2}\right)}\left(\sigma_{e_1} + \sigma_{e_2}\right) \tag{7}$$

$$\Delta p_{res-thr} = \frac{1}{\dot{s}\left(\frac{p_1+p_2}{2}\right)}\sqrt[4]{\frac{4}{\left(\hat{\kappa}_1^2 - \frac{1}{N}\right)}}\left(\sqrt{\sigma_{e_1}} + \sqrt{\sigma_{e_2}}\right) \tag{8}$$

where p represents a directional parameter, such as θ, ϕ or cone angles. $\dot{s}\,(p)$ is the rate of change of manifold arc length at point p and κ_1 is the manifold's principal curvature (where $\hat{\kappa}_1$ also takes into account the inclination angle of the manifold). For a parameterisation in terms of θ, these properties of the manifold are related to familiar system parameters as follows [3]:

$$\dot{s}\,(\theta) = \pi \cos(\phi)\,\|\underline{R}_\theta\| \tag{9}$$

$$\kappa_1\,(\theta) \approx \left\|\widetilde{\underline{R}}_\theta\right\|^2 \tag{10}$$

$$\hat{\kappa}_1\,(\theta) = \sqrt{\kappa_1^2\,(\theta) - \left|\underline{1}_N^T \widetilde{\underline{R}}_\theta^3\right|^2} \tag{11}$$

where $\underline{R}_\theta \triangleq \left(\underline{r}_y \cos(\theta) - \underline{r}_x \sin(\theta)\right)$ and $\widetilde{\underline{R}}_\theta \triangleq \frac{\underline{R}_\theta}{\|\underline{R}_\theta\|}$.

This paper is concerned specifically with the theoretically minimum resolvable source separation (Equation 8) and how close different practical algorithms - under the same conditions - come to achieving it. A typical superresolution DF null spectrum showing a source separation close to resolution threshold is shown in Figure 2:

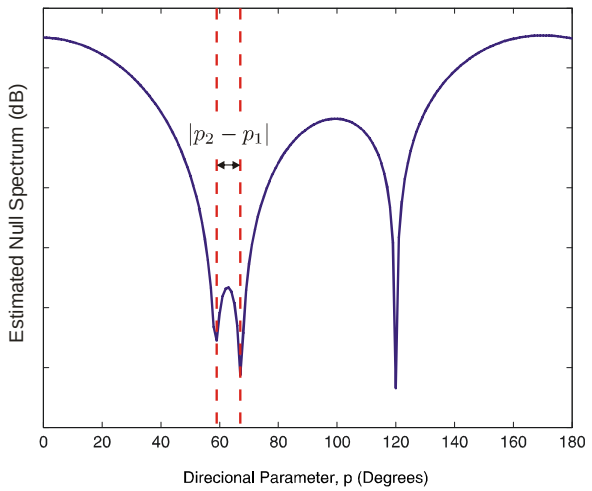

Fig. 2: A typical estimated DOA null spectrum, showing three successfully-resolved sources at the three distinct nulls. Resolution is considered between the two closely-spaced sources.

IV. Algorithm-specific Expressions for C

By substituting the algorithm-specific resolution threshold expressions given in Appendix A into the expressions for ideal resolution performance derived in Appendices B and C, the main results of this paper are now presented. Specifically, the C parameters for MUSIC, Minimum Norm and optimum Beamspace MUSIC are given in Equations 11-14, below. In these expressions, $\frac{P_2}{P_1}$ is the ratio of the two closely-spaced sources' powers, d_r is sensor spacing in units of $\frac{\lambda}{2}$, $\breve{\theta} \triangleq \frac{\theta_1+\theta_2}{2}$ is the midpoint between the two sources and $\Delta^2 \triangleq \frac{1}{N}\left\|\mathbf{r}\left(\underline{k}\left(\theta_2\right)-\underline{k}\left(\theta_1\right)\right)\right\|^2$ is a geometry-dependent separation measure. $\xi_{music}\left(\theta\right) \triangleq \underline{S}(\theta)^H \mathbb{E}_n \mathbb{E}_n^H \underline{S}(\theta)$ is the MUSIC null spectrum [4], with the columns of $\mathbb{E}_n$ given by the eigenvectors associated with the $(N-M)$ smallest eigenvalues of the observed signal's theoretical covariance matrix.

Note that Equations 11 and 12 apply only to a uniform linear array (ULA) and equipower sources, while Equations 13 and 14 are valid for unequal source powers and arbitrary array geometry. The approximate expression of Equation 12 is only valid for sufficiently small separations (such that Equation 11 is dominated by the $1/\left(N-2\right)$ term).

A. Discussion

As discussed in [6], optimal Beamspace MUSIC is defined by the beamforming preprocessor, $\mathbb{B}_{opt}$, which maximises resolution performance. Applying the matrix $\mathbb{B}_{opt}$ to the received data snapshots before any eigenspace-based technique (such as MUSIC or Minimum Norm) yields the same 'optimal' resolution performance. Since $\mathbb{B}_{opt}$ is independent of $\frac{P_2}{P_1}$, it follows that the effect of $\frac{P_2}{P_1}$ on resolution performance will be the same for all eigenspace-based algorithms[1]. Specifically, it is evident from Equations 13 and 14 that $\frac{P_2}{P_1}$ causes performance degradation relative to the equipower case, approximately given by:

$$C_{eigenspace} \approx \frac{\left(1+\sqrt[4]{\frac{P_2}{P_1}}\right)^4}{8\left(3-\frac{P_2}{P_1}\right)} C_{\substack{eigenspace \\ given\ \frac{P_2}{P_1}=1}} \tag{15}$$

which can be approximated by:

$$C_{eigenspace} \approx \frac{\left(4+21\frac{P_2}{P_1}\right)}{25} \times C_{\substack{eigenspace \\ given\ \frac{P_2}{P_1}=1}}$$

for $\frac{P_2}{P_1} \gtrsim 0.05$.

From Equations 11-13, it can be seen that MUSIC (with arbitrary array geometry) and Minimum Norm (ULA geometry) can both exhibit near-ideal performance for 3-element arrays when $\frac{P_2}{P_1}=1$. However, optimal Beamspace MUSIC can also achieve near-ideal resolution performance for larger arrays ($N>3$), when $\frac{P_2}{P_1}=1$ and the following condition holds:

$$\frac{16L\xi_{music}\left(\breve{\theta}\right)}{N\Delta^2} \ll 1 \tag{16}$$

Since, as is shown in Appendix B, $\xi_{music}\left(\breve{\theta}\right)$ is proportional to both $\dot{s}\left(\breve{\theta}\right)^4$ (which grows rapidly with increasing N) and $\left|\theta_2-\theta_1\right|^4$, this condition generally holds for small L, N and $|\theta_2-\theta_1|$. In Figure 3, the C parameters for the three algorithms are compared for ULAs with increasing numbers of sensors.

In Figure 4, the variation of C as a function of azimuth is shown (where the shape of the plot depends on the array geometry).Optimum Beamspace MUSIC clearly exhibits the best resolution performance, but its superiority is less outstanding for larger source separations. The same effect can also be observed for larger numbers of snapshots.

A general trend is that these algorithms perform closer to the ideal when N, L and $|\theta_2-\theta_1|$ are restricted, but there may be

[1]Proof of these conditions and a detailed discussion of how to obtain $\mathbb{B}_{opt}$ are given in [6].

$$C_{music} = \frac{1}{(N-2)} \frac{2}{\left[1+\sqrt{1+\frac{L(N+2)(\pi d_r|\cos\theta_2-\cos\theta_1|)^2}{60}}\right]} \text{ (only for ULA with } P_1=P_2) \tag{11}$$

$$C_{min\_norm} \approx \frac{5}{(N+2)} \text{ (only for ULA with } P_1=P_2) \tag{12}$$

$$C_{music} = \frac{\left(1+\sqrt[4]{\frac{P_2}{P_1}}\right)^4}{8\left(3-\frac{P_2}{P_1}\right)(N-2)} \frac{2}{\left[1+\sqrt{1+\frac{16\left(1+\frac{P_2}{P_1}\right)L\xi_{music}\left(\breve{\theta}\right)}{\left(3-\frac{P_2}{P_1}\right)N(N-2)\Delta^2}}\right]} \tag{13}$$

$$C_{opt\_beamspace} = \frac{\left(1+\sqrt[4]{\frac{P_2}{P_1}}\right)^4}{8\left(3-\frac{P_2}{P_1}\right)} \frac{2}{\left[1+\sqrt{1+\frac{16\left(1+\frac{P_2}{P_1}\right)L\xi_{music}\left(\breve{\theta}\right)}{\left(3-\frac{P_2}{P_1}\right)N\Delta^2}}\right]} \tag{14}$$

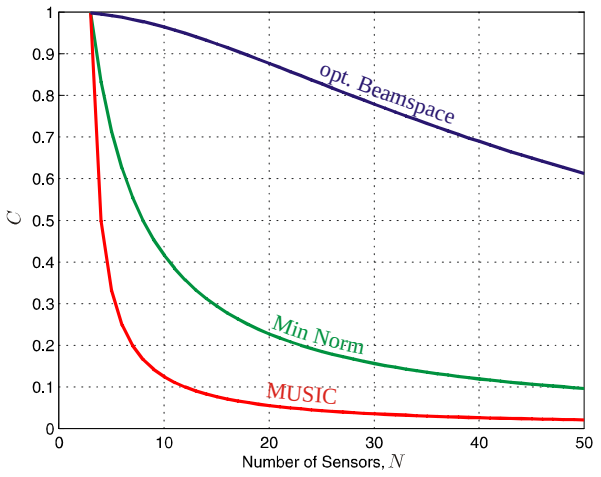

Fig. 3: $C_{opt\_beamspace}$, C_{min_norm} and C_{music} as a function of the number of sensors, N, for a ULA. In each case, $\theta_1 = 34°$, $\theta_2 = 35°$, $\frac{P_2}{P_1} = 1$ and $L = 100$.

considerable scope for improvement by future algorithms that can better utilise the greater resolving capacity of the system as these quantities increase.

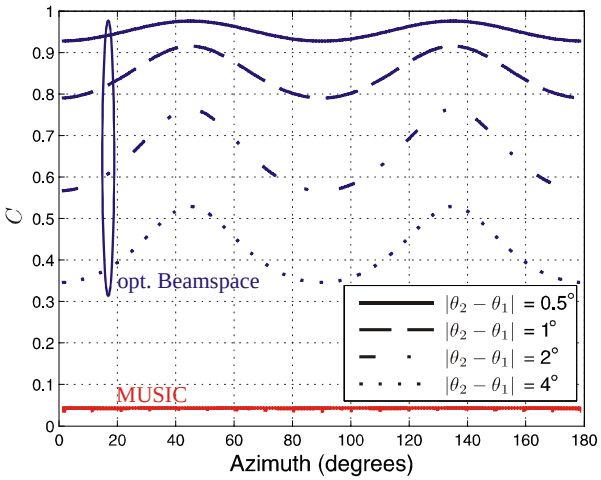

Fig. 4: $C_{opt\_beamspace}$ and C_{music} for various source separations (for a 25-element uniform X-shaped array) with $\frac{P_2}{P_1} = 1$ and $L = 100$. Since C_{music} is relatively insensitive to changes in $|\theta_2 - \theta_1|$, the separate traces cannot be distinguished.

B. A Note on Correlated Signals

Our discussion so far has considered only uncorrelated signals. In practice, signals are often correlated (particularly in multipath signal environments and in applications such as radar/sonar) and it is well-known that this can severely degrade resolution performance. A popular method of 'decorrelating' signals is spatial smoothing [10]. In [11], it is shown that, for two equipowered, fully-correlated (coherent) sources impinging on a ULA, the resolution performance of the forward-backward spatially-smoothed MUSIC algorithm is worse by a factor of approximately $4\left(N\pi d_r\left|\cos\theta_2 - \cos\theta_1\right|\right)^{-2}$, compared to the standard, uncorrelated case.

V. Conclusion

In this paper, the parameter C has been proposed as a figure of merit for comparing superresolution DF algorithms. Representative examples were derived for the MUSIC, optimal Beamspace MUSIC and Minimum Norm algorithms (for uncorrelated signals). It was found that, when sources have equal powers, all these algorithms can offer near-ideal resolution performance for 3-element arrays. However, only optimum Beamspace MUSIC can achieve this for larger arrays.

In general, the greatest scope for improvement by future superresolution algorithms would be available to those which can better utilise the greater resolving capacity of the system as the number of sensors, number of snapshots and source separations increase.

Appendix

A. Algorithm-specific Resolution Threshold Expressions

In this Appendix, analytical expressions are derived for the parameter C for MUSIC, optimal Beamspace MUSIC and Minimum Norm. In order to do this, in each case, an algorithm-specific resolution threshold expression is first required. Specifically, the results first derived in [5-9] will be used.

In order to match the conventions of algorithm-specific threshold expressions found in the literature, it is constructive to express the theoretically ideal resolution performance of Equation 8 in terms of $(\mathrm{SNR} \times L)$:

$$(\mathrm{SNR}_2 \times L)_{res} = \frac{2}{\Delta p^4 \dot{s}\left(\frac{p_1+p_2}{2}\right)^4\left(\hat{\kappa}_1^2 - \frac{1}{N}\right)C}\left(1 + \sqrt[4]{\frac{P_2}{P_1}}\right)^4 \quad (17)$$

Resolution threshold expressions for each algorithm will now be considered and compared to Equation 17.

Following a small modification[2], the resolution threshold for the MUSIC algorithm (first derived by Kaveh and Barabell in [5]) is shown in Equation 18. It is valid for two equipower, uncorrelated sources impinging on a uniform linear array (ULA).

In the literature, several attempts to derive the equivalent threshold condition for the Minimum Norm algorithm can be found. However, these analyses yield different results[3]. In the absence of a single, widely-accepted threshold expression, it is

[2]Since the resolution threshold expression given in [5] implies above-ideal performance for sufficiently small N, we replace [5, Equation B.1] with a more accurate Taylor expansion. The resulting threshold expression then agrees with [7].

[3]In [7], an improvement in resolution performance over MUSIC by a factor of approximately $5\frac{(N-1)(N-2)}{(N-3)(N+2)}$ is suggested. Meanwhile, a factor of about $5\frac{(N-2)}{(N+2)}$ can be found in [8]. A similar (but not identical) improvement of approximately $5\frac{(N-2)}{(N+2)}$ is also found in [9].

$$(SNR \times L)_{music}^{(ULA,P_1=P_2)} = \frac{2880\left(\pi d_r \left|\cos\theta_2 - \cos\theta_1\right|\right)^{-4}}{N(N^2-1)(N+2)} \left[1 + \sqrt{1 + \frac{L(N+2)\left(\pi d_r \left|\cos\theta_2 - \cos\theta_1\right|\right)^2}{60}}\right] \quad (18)$$

simply considered here that Minimum Norm's resolution performance is superior to MUSIC's, according to the following approximate relationship:

$$(\mathrm{SNR} \times L)_{min\_norm} \approx \frac{(N+2)}{5\,(N-2)} (\mathrm{SNR} \times L)_{music} \quad (19)$$

The above expressions are valid only for equipower sources and ULAs. However, the following threshold expressions (derived by Lee and Wengrovitz in [6]) are valid for unequal source powers and arbitrary array geometry:

$$(\mathrm{SNR}_2 \times L)_{music} = \frac{\left(3 - \frac{P_2}{P_1}\right)(N-2)}{8\xi_{music}\left(\breve{\theta}\right)} \left[1 + \sqrt{1 + \frac{16\left(1 + \frac{P_2}{P_1}\right) L\xi_{music}\left(\breve{\theta}\right)}{\left(3 - \frac{P_2}{P_1}\right)(N-2)\,\Delta^2}}\right] \quad (20)$$

$$(\mathrm{SNR}_2 \times L)_{opt\_beamspace} = \frac{\left(3 - \frac{P_2}{P_1}\right)}{8\xi_{music}\left(\breve{\theta}\right)} \left[1 + \sqrt{1 + \frac{16\left(1 + \frac{P_2}{P_1}\right) L\xi_{music}\left(\breve{\theta}\right)}{\left(3 - \frac{P_2}{P_1}\right)\Delta^2}}\right] \quad (21)$$

It should be noted that Equation 17 shows dependency on properties of the differential geometry of the array manifold. In order to obtain compact expressions for C, Equation 17 must therefore first be manipulated into a more amenable form. As shown in Appendix B, this task is simplified significantly by first restricting analysis to the ULA geometry. Furthermore, in Appendix C, Equation 17 is expressed in terms of $\xi_{music}\left(\breve{\theta}\right)$ for arbitrary array geometry.

B. Ideal Resolution Performance for ULA

For a ULA with its phase centre taken to be its centroid (with antenna spacing d_r), the sensor locations are given by:

$$\underline{r}_x = d_r \left[-\frac{(N-1)}{2}, -\frac{(N-1)}{2} + 1, \ldots, \frac{(N-1)}{2}\right]^T \quad (22)$$

Using the method of finite differences, it is easily shown that:

$$\|\underline{r}_x\| = \frac{d_r}{\sqrt{12}}\sqrt{(N^3 - N)} \quad (23)$$

Then, using this result, we similarly find:

$$\kappa_1 = \left\| \frac{\underline{r}_x}{\|\underline{r}_x\|} \odot \frac{\underline{r}_x}{\|\underline{r}_x\|} \right\| = \sqrt{\frac{3(3N^2-7)}{5(N^3-N)}} \quad (24)$$

For symmetric linear arrays, $\hat{\kappa}_1 = \kappa_1$. Substituting Equations 23 and 24 into Equation 17 and setting $\frac{P_2}{P_1} = 1$ then yields:

$$(\mathrm{SNR}_2 \times L)_{res} = \frac{5760\left(\pi d_r \left|\cos\theta_2 - \cos\theta_1\right|\right)^{-4}}{N\,(N^2-1)\,(N^2-4) \times C} \quad (25)$$

C. Ideal Resolution Performance in Terms of $\xi_{music}\left(\breve{\theta}\right)$

It can be shown, using the circular approximation of the array manifold, that the spectral midpoint in the MUSIC spectrum can be approximated by:

$$\xi_{music}\left(\breve{\theta}\right) \approx \frac{\left(\hat{\kappa}_1^2 - \frac{1}{N}\right)\Delta p^4 \dot{s}\left(\frac{p_1+p_2}{2}\right)^4}{64} \quad (26)$$

Although the proof of Equation 26 cannot be included here due to space restrictions, note that it follows somewhat intuitively from Equations 11, 20 and 21. That is, the resolution performance of optimal Beamspace MUSIC is better than standard (sensor-space) MUSIC's by a factor of approximately $(N-2)$. According to Equation 11, this would yield near-ideal resolution performance for a ULA with $\frac{P_2}{P_1} = 1$. Since $\xi_{music}\left(\breve{\theta}\right)$ contains the effects of arbitrary array geometry, $C_{music} \approx 1/(N-2)$ holds for arbitrary array geometry and so comparing $\frac{\left(3-\frac{P_2}{P_1}\right)}{4\xi_{music}\left(\breve{\theta}\right)}$ to Equation 17 with $\frac{P_2}{P_1} = 1$ yields the same result:

$$(\mathrm{SNR}_2 \times L)_{res} = \frac{\left(1 + \sqrt[4]{\frac{P_2}{P_1}}\right)^4}{32\xi_{music}\left(\breve{\theta}\right) \times C} \quad (27)$$

REFERENCES

[1] H. Krim and M. Viberg, "Two Decades of Array Signal Processing Research: The Parametric Approach", IEEE Signal Processing Magazine, pp. 67-94, July 1996.

[2] A. Manikas, "Differential Geometry in Array Processing", Imperial College Press, 2004.

[3] A. Manikas, A. Alexiou and H. Karimi, "Comparison of the Ultimate Direction-finding Capabilities of a Number of Planar Array Geometries", IEE Proc. Radar, Sonar, Navig., vol. 144, No. 6, pp. 321-329, 1997.

[4] R.O. Schmidt, "Multiple Emitter Location and Signal Parameter Estimation", IEEE Trans. Antennas Propagation, Vol. 34, pp.276-280, 1986.

[5] M. Kaveh and A.J. Barabell, "The statistical performance of the MUSIC and minimum-norm algorithm in resolving plane waves in noise". IEEE Trans. Acoust. Speech Signal Process. Vol. 34 , pp. 331–341, Apr. 1986.

[6] H. Lee and M. Wengrovitz, "Resolution threshold of beamspace MUSIC for two closely spaced emitters", IEEE Trans. Acoustics Speech Signal Process. 38, pp. 1545–1559, 1990.

[7] P. Tichavsky, "Estimating the angles of arrival of multiple plane waves: The statistical performance of the MUSIC and the Minimum Norm Algorithm", Kybernetika, vol. 24, no. 3, pp. 196-206, 1988.

[8] J. Luo and Z. Bao, "The Resolution Performance of Eigenstructure Approach" [Chinese], Journal of Electronics, vol. 13, no. 4, 1991.

[9] P. Forster and E. Villier, "Simplified formulas for performance analysis of MUSIC and Min Norm", OCEANS'98, Nice, France, 1998.

[10] T.J. Shan, M. Wax and T. Kailath, "On Spatial Smoothing for Direction of Arrival Estimation of Coherent Signals", IEEE Trans. Acoust. Speech Signal Process., Vol. 33, pp. 806-811, 1985.

[11] U. Pillai and B. Kwon, "Performance analysis of MUSIC-type high resolution estimators for direction finding in correlated and coherent scenes," IEEE Trans. ASSP, vol. 37, no. 8, pp. 1176-1189, 1989.